

The reaction $e^+e^- \rightarrow e^+e^-\pi^+\pi^-$ and the pion form factor measurements via the radiative return method ^{*}

Henryk Czyż, Elżbieta Nowak-Kubat

Institute of Physics, University of Silesia, PL-40007 Katowice, Poland.

Abstract

The role of the reaction $e^+e^- \rightarrow e^+e^-\pi^+\pi^-$ in the pion form factor measurements via radiative return method without photon tagging is studied in detail. The analysis is based on the developed Monte Carlo program EKHARA, which ingredients are also presented.

Key words: radiative return, pair production, pion form factor

PACS: 13.40.Ks,13.66.Bc

1 Introduction

Radiative return method of the hadronic cross section extraction from the measurement of the cross section of the reaction $e^+e^- \rightarrow \text{hadrons} + \text{photon(s)}$, proposed already some time ago [1], is currently being used by KLOE [2] and BaBar [3] providing very precise experimental data. Further improvement in accuracy is crucial for predictions of the hadronic contributions to a_μ , the anomalous magnetic moment of the muon, as the error on the hadronic contributions to a_μ may obscure possible new physics signal, seen as a deviation from the Standard Model (SM) predictions. The same information is essential for the evaluation of the running of the electromagnetic coupling (α_{QED}) from its value at low energy up to M_Z as the present error on the hadronic

^{*} Work supported in part by EC 5-th Framework EURIDICE network project HPRN-CT2002-00311, TARI project RII3-CT-2004-506078 and Polish State Committee for Scientific Research (KBN) under contract 1 P03B 003 28.

contributions is too big to fully profit from the data of the future ILC (International Linear Collider) running in the gigaZ mode. For recent reviews of these subjects look [4,5,6].

The extraction of the cross section $\sigma(e^+e^- \rightarrow \text{hadrons})$ from the measured cross section $\sigma(e^+e^- \rightarrow \text{hadrons} + \text{photons})$ relies on the factorization

$$d\sigma(e^+e^- \rightarrow \text{hadrons} + n\gamma) = H d\sigma(e^+e^- \rightarrow \text{hadrons}) , \quad (1)$$

valid at any order for photons emitted from initial leptons, where the function H contains QED radiative corrections. This function is known analytically, if no cuts are imposed, at next to leading order (NLO) and has to be provided in form of an event generator [7,8] of the reaction $e^+e^- \rightarrow \text{hadrons} + \text{photons}$ for a realistic experimental setup.

Let us focus on the most important process, where the 'hadrons' means just $\pi^+\pi^-$ pair. This reaction gives the dominant contribution to the hadronic part of a_μ as well as to its error. In case the photon(s) are not measured and only charged pions are tagged, there exists a number of possible backgrounds. It was pointed out in [9], basing on integrated over the whole phase space analytical formulae and containing contributions from diagrams (a) and (d) in Fig.1, that the reaction $e^+e^- \rightarrow e^+e^-\pi^+\pi^-$ can give sizable contributions to the radiative return process, especially for low invariant masses of two pion system. To examine this contribution for a realistic experimental setup, a Monte Carlo program EKHARA was developed. It is the scope of this letter to present its ingredients and results of the simulations relevant for the pion form factor extraction via the radiative return method.

Some partial results concerning the electron-positron pair production contributions to the pion form factor measurements and tests of the code were presented in [10,11], while in this letter the amplitude describing the reaction $e^+e^- \rightarrow e^+e^-\pi^+\pi^-$ is discussed, generation procedure is described in detail and results based on the complete tree level amplitude are presented.

2 The scattering amplitude and the generation procedure

As stated already in the introduction, the reaction $e^+e^- \rightarrow e^+e^-\pi^+\pi^-$ plays a role in the pion form factor measurement via the radiative return method only if the photons in the reaction $e^+e^- \rightarrow \pi^+\pi^- + \text{photons}$ are not tagged. This version of the radiative return method was used already by KLOE [2] and as more accurate analysis, based on a significantly bigger data sample, is expected, a detailed study of all possible contributions is obligatory. The

complete set of the lowest order diagrams, describing the reaction $e^+e^- \rightarrow e^+e^-\pi^+\pi^-$, is shown schematically in Fig.1.

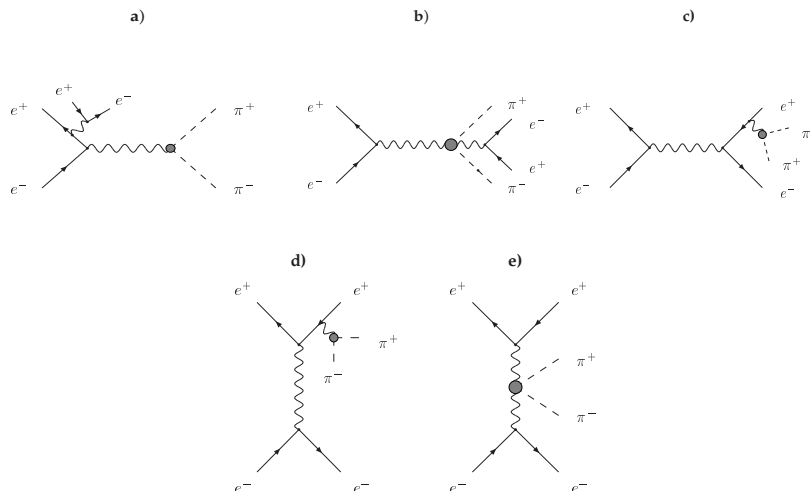


Fig. 1. Diagrams contributing to the process $e^+(p_1)e^-(p_2) \rightarrow \pi^+(\pi_1)\pi^-(\pi_2)e^+(q_1)e^-(q_2)$: initial state pair emission (a), final state pair emission (b,c), pion pair emission from t-channel Bhabha process (d) and $\gamma^*\gamma^*$ pion pair production (e). Only one representative diagram for a given set of diagrams is shown.

Helicity amplitude method, with the conventions described in [12,13], was used for the scattering amplitude evaluation. It allows for a fast numerical evaluation and, in addition, all interferences are easily included. Moreover, it partly avoids numerical cancellations present, when one uses the trace method to get the square of the amplitude. To model photon-pion interactions, we use scalar QED (sQED) combined with the vector dominance model (VDM). Within these assumptions, the amplitude has the form

$$M = M_a + M_b + M_c + M_d + M_e, \quad (2)$$

where the amplitudes M_i , $i = a, \dots, e$ correspond to the contributions from the diagrams (a)-(e) from Fig.1. They read

$$M_a = -\frac{ie^4}{k_1^2 Q^2} \bar{u}(q_2) \gamma_\mu v(q_1) \cdot \bar{v}(p_1) \left(\frac{(\gamma^\mu \not{k}_1 - 2p_1^\mu) \not{F}}{k_1^2 - 2k_1 \cdot p_1} + \frac{\not{F}(2p_2^\mu - \not{k}_1 \gamma^\mu)}{k_1^2 - 2k_1 \cdot p_2} \right) u(p_2) \quad (3)$$

$$M_b = \frac{-2ie^4 F(s)}{sk_1^2} \bar{v}(p_1) \gamma_\mu u(p_2) \cdot \bar{u}(q_2) \left(\gamma^\mu + \frac{2\pi_2^\mu \not{\eta}_1}{k_1^2 + 2\pi_1 \cdot k_1} + \frac{2\pi_1^\mu \not{\eta}_2}{k_1^2 + 2\pi_2 \cdot k_1} \right) v(q_1) \quad (4)$$

$$M_c = \frac{ie^4}{sQ^2} \bar{u}(q_2) \left(\frac{\gamma^\mu (\not{V}Q - 2q_1 \cdot \Gamma)}{Q^2 + 2Q \cdot q_1} + \frac{(\not{V}Q + 2q_2 \cdot \Gamma) \gamma^\mu}{Q^2 + 2Q \cdot q_2} \right) v(q_1) \cdot \bar{v}(p_1) \gamma_\mu u(p_2) \quad (5)$$

$$M_d = \frac{ie^4}{tQ^2} \bar{v}(p_1) \left(\frac{(\not{V}Q - 2p_1 \cdot \Gamma) \gamma^\mu}{Q^2 - 2Q \cdot p_1} + \frac{\gamma^\mu (\not{V}Q - 2q_1 \cdot \Gamma)}{Q^2 + 2Q \cdot q_1} \right) v(q_1) \cdot \bar{u}(q_2) \gamma_\mu u(p_2) \\ - \frac{ie^4}{t_1 Q^2} \bar{u}(q_2) \left(\frac{\gamma^\mu (2p_2 \cdot \Gamma - \not{Q})}{Q^2 - 2Q \cdot p_2} + \frac{(2q_2 \cdot \Gamma + \not{V}Q) \gamma^\mu}{Q^2 + 2Q \cdot q_2} \right) u(p_2) \bar{v}(p_1) \gamma_\mu v(q_1) \quad (6)$$

$$M_e = \frac{-2ie^4 F(t) F(t_1)}{tt_1} \left(\bar{v}(p_1) \gamma^\mu v(q_1) \bar{u}(q_2) \gamma_\mu u(p_2) \right. \\ \left. + \frac{2\bar{v}(p_1) \not{k}_1 v(q_1) \bar{u}(q_2) \not{k}_2 u(p_2)}{t_1 - 2\pi_1(p_1 - q_1)} + \frac{2\bar{v}(p_1) \not{k}_2 v(q_1) \bar{u}(q_2) \not{k}_1 u(p_2)}{t + 2\pi_1(q_2 - p_2)} \right), \quad (7)$$

where

$$\Gamma^\mu = F(Q^2) (\pi_1 - \pi_2)^\mu, \quad k_1 = q_1 + q_2, \quad Q = \pi_1 + \pi_2, \quad (8)$$

$$s = (p_1 + p_2)^2, \quad t = (q_2 - p_2)^2, \quad t_1 = (p_1 - q_1)^2 \quad (9)$$

and $F(Q^2)$ is the pion form factor, which was adopted from [14]. For the numerical evaluation, following again the method described in papers [12,13], the amplitude is rewritten into a form where only 2x2 matrices appear.

We use the multi-channel variance reduction method to improve efficiency of the generator and the generation is split into four channels, where two of them absorb peaks present in t-channel diagrams and other two take care of the s-channel peaks.

For the t-channel peaks absorption, we use the following phase space representation

$$d\text{Lips}_4(p_1 + p_2; q_1, q_2, \pi_1, \pi_2) = \\ d\text{Lips}_2(p_1 + p_2; Q', q_2) \frac{dQ'^2}{2\pi} d\text{Lips}_2(Q'; Q, q_1) \frac{dQ^2}{2\pi} d\text{Lips}_2(Q; \pi_1, \pi_2) \quad (10)$$

in one of the channels and an analogous one, with $q_1 \leftrightarrow q_2$, in the other channel. As both channels are completely symmetric under $q_1 \leftrightarrow q_2$, we will describe here only changes of variables, which smoothen the distribution, only in one of them. For the two invariant masses (Q^2 and Q'^2) the following change of variables was performed

$$Q^2 = (\sqrt{s} - 2m_e - \sqrt{-2z})^2, \quad z = -\frac{1}{2}(\sqrt{s} - 2m_e - 2m_\pi)^2(1 - r_{Q^2}), \quad (11)$$

$$Q'^2 = \frac{1}{\sqrt[3]{-3y}} + m_e^2, \quad (12)$$

$$y = -\frac{1}{3(Q^2 + 2\sqrt{Q^2}m_e)^3} + \left(\frac{1}{3(Q^2 + 2\sqrt{Q^2}m_e)^3} - \frac{1}{3(s - 2\sqrt{sm_e})^3} \right) r_{Q'^2}.$$

The angles of \bar{q}_2 vector are defined in the initial e^+e^- center of mass (cms) frame with z-axis along \bar{p}_1 and the polar angle is used to absorb the peak coming from the propagator of the photon exchanged in the t -channel

$$\cos \theta_{q_2} = \frac{3m_e^2 - s + Q'^2 - 2t}{\sqrt{1 - \frac{4m_e^2}{s}\lambda^{1/2}(s, Q'^2, m_e^2)}}, \quad t = -\frac{1}{y},$$

$$y = -\frac{1}{t_-} + \frac{s\sqrt{1 - \frac{4m_e^2}{s}\lambda^{1/2}(s, Q'^2, m_e^2)}}{m_e^2(Q'^2 - m_e^2)^2} r_{\theta_{q_2}}, \quad \phi_{q_2} = 2\pi r_{\phi_{q_2}}, \quad (13)$$

where

$$t_- = \frac{1}{2} \left(3m_e^2 - s + Q'^2 - \sqrt{1 - \frac{4m_e^2}{s}\lambda^{1/2}(s, Q'^2, m_e^2)} \right). \quad (14)$$

The angles of the \bar{Q} vector are defined in Q' rest frame and the appropriate change of variables reads

$$\cos \theta_Q = \frac{2E'_1 Q_0 - Q^2 - \frac{1}{2|\vec{p}'_1||\bar{Q}|x}}{2|\vec{p}'_1||\bar{Q}|}, \quad \phi_Q = 2\pi r_{\phi_Q} \quad (15)$$

$$x = \frac{-1}{2|\vec{p}'_1||\bar{Q}|(Q^2 - 2E'_1 Q_0 - 2|\vec{p}'_1||\bar{Q}|)} + \frac{2}{(Q^2 - 2E'_1 Q_0)^2 - 4|\vec{p}'_1|^2|\bar{Q}|^2} r_{\theta_Q},$$

where $E'_1 = \frac{Q'^2 - t + m_e^2}{2\sqrt{Q'^2}}$, $Q_0 = \frac{Q'^2 + Q^2 - m_e^2}{2\sqrt{Q'^2}}$, $|\vec{p}'_1| = \frac{\lambda^{1/2}(Q'^2, t, m_e^2)}{2\sqrt{Q'^2}}$, $|\bar{Q}| = \frac{\lambda^{1/2}(Q'^2, Q^2, m_e^2)}{2\sqrt{Q'^2}}$ and $\lambda(a, b, c) = a^2 + b^2 + c^2 - 2(ab + ac + bc)$. As we chose here the z-axis along the \vec{p}'_1 (the \bar{p}_1 in the Q' rest frame) the vectors have to be rotated after generation to restore the general choice of the z-axis along \bar{p}_1 in the e^+e^- cms frame.

Finally the angles of the positively charged pion are generated in the Q rest frame with flat distributions

$$\cos \theta_{\pi_1} = -1 + 2r_{\theta_{\pi_1}} , \quad \phi_{\pi_1} = 2\pi r_{\phi_{\pi_1}} . \quad (16)$$

The described change of variables transforms the phase space into a unit hypercube ($0 < r_i < 1$, $i = Q^2, \dots, \phi_{\pi_1}$) and collecting all the jacobians it reads

$$d\text{Lips}_4(p_1 + p_2; q_1, q_2, \pi_1, \pi_2) = P(q_1, q_2) dr_{Q^2} dr_{Q'^2} dr_{\theta_{q_2}} dr_{\phi_{q_2}} dr_{\theta_Q} dr_{\phi_Q} dr_{\theta_{\pi_1}} dr_{\phi_{\pi_1}} \quad (17)$$

with

$$P(q_1, q_2) = \frac{1}{6(4\pi)^5 Q'^2 m_e^2} \lambda^{1/2}(Q'^2, Q^2, m_e^2) \lambda^{1/2}(s, Q'^2, m_e^2) \sqrt{1 - \frac{4m_\pi^2}{Q^2}} \\ \frac{t^2 (Q'^2 - m_e^2)^2 (Q^2 - 2Q \cdot p_1)^2}{(Q^2 - 2E'_1 Q_0)^2 - 4|p'_1|^2 |\bar{Q}|^2} \frac{\sqrt{Q^2}(\sqrt{s} - 2m_e - 2m_\pi)^2}{\sqrt{s} - 2m_e - \sqrt{Q^2}} \\ \left(\frac{1}{(Q^2 + 2\sqrt{Q^2}m_e)^3} - \frac{1}{(s - 2\sqrt{sm_e})^3} \right) . \quad (18)$$

For the s -channel generation it is convenient to write the phase space in the following form

$$d\text{Lips}_4(p_1 + p_2; q_1, q_2, \pi_1, \pi_2) = \\ d\text{Lips}_2(p_1 + p_2; Q, k_1) \frac{dk_1^2}{2\pi} d\text{Lips}_2(k_1; q_1, q_2) \frac{dQ^2}{2\pi} d\text{Lips}_2(Q; \pi_1, \pi_2) . \quad (19)$$

The two generation channels used here differ only in the generation of the electron–positron pair invariant mass k_1^2 and the change of variables will be described simultaneously. The invariant mass Q^2 is generated with a flat distribution

$$Q^2 = 4m_\pi^2 + ((\sqrt{s} - 2m_e)^2 - 4m_\pi^2)r_{Q^2} . \quad (20)$$

Reflecting two leading k_1^2 behaviours of the cross section, two distinct changes of variables are done in the generation of k_1^2 :

$$k_1^2 = s \exp(y_I^{1/3}) , \quad (21) \\ y_I = \ln^3(4m_e^2/s) + \left[\ln^3 \left(\left(1 - \sqrt{Q^2/s} \right)^2 \right) - \ln^3(4m_e^2/s) \right] r_{k_1^2, I}$$

$$\begin{aligned}
k_1^2 &= s(1 - \exp(-y_{II})) , \\
y_{II} &= -\ln(1 - 4m_e^2/s) - \ln\left(\frac{\sqrt{Q^2}(2\sqrt{s} - \sqrt{Q^2})}{(s - 4m_e^2)}\right) r_{k_1^2, II} .
\end{aligned} \tag{22}$$

The \bar{k}_1 polar angle is used to absorb peaks coming from the electron propagator, while its azimuthal angle is generated with a flat distribution:

$$\begin{aligned}
\phi_{k_1} &= 2\pi r_{\phi_{k_1}} , \quad \cos \theta_{k_1} = \frac{-k_1^2 + 2k_{10}p_{10}}{2|\bar{k}_1||\bar{p}_1|} \tanh\left(\frac{y}{2}\right) \\
y &= \ln\left(\frac{k_1^2 - 2k_{10}p_{10} + 2|\bar{k}_1||\bar{p}_1|}{k_1^2 - 2k_{10}p_{10} - 2|\bar{k}_1||\bar{p}_1|}\right) + \ln\left(\frac{k_1^2 - 2k_{10}p_{10} - 2|\bar{k}_1||\bar{p}_1|}{k_1^2 - 2k_{10}p_{10} + 2|\bar{k}_1||\bar{p}_1|}\right)^2 r_{\theta_{k_1}} ,
\end{aligned} \tag{23}$$

where $k_{10} = \frac{s+k_1^2-Q^2}{2\sqrt{s}}$, $p_{10} = \frac{\sqrt{s}}{2}$, $|\bar{p}_1| = \sqrt{\frac{s}{4} - m_e^2}$ and $|\bar{k}_1| = \frac{\lambda^{1/2}(s, k_1^2, Q^2)}{2\sqrt{s}}$, are defined in the $p_1 + p_2$ rest frame.

The \bar{q}_1 and the $\bar{\pi}_1$ angles are generated with flat distributions

$$\phi_{q_1} = 2\pi r_{\phi_{q_1}} , \quad \cos \theta_{q_1} = -1 + 2r_{\theta_{q_1}} , \quad \phi_{\pi_1} = 2\pi r_{\phi_{\pi_1}} , \quad \cos \theta_{\pi_1} = -1 + 2r_{\theta_{\pi_1}} . \tag{24}$$

After the described changes of variables are performed, the phase space reads ($i = I$ or II)

$$d\text{Lips}_4(p_1 + p_2; q_1, q_2, \pi_1, \pi_2) = P_{s,i} dr_{k_1^2} dr_{Q^2} dr_{\theta_{k_1}} dr_{\phi_{k_1}} dr_{\theta_{q_1}} dr_{\phi_{q_1}} dr_{\theta_{\pi_1}} dr_{\phi_{\pi_1}} , \tag{25}$$

with

$$\begin{aligned}
P_{s,i} &= \frac{1}{4(4\pi)^5 s} \sqrt{1 - \frac{4m_\pi^2}{Q^2}} \sqrt{1 - \frac{4m_e^2}{k_1^2}} \lambda^{1/2}(s, Q^2, k_1^2) \left((\sqrt{s} - 2m_e)^2 - 4m_\pi^2 \right) \\
&\cdot \frac{|\bar{k}_1||\bar{p}_1|}{2k_{10}p_{10} - k_1^2} \left(\frac{-k_1^2 + 2k_{10}p_{10}}{2|\bar{k}_1||\bar{p}_1|} - \cos \theta_{k_1} \right) \left(\frac{-k_1^2 + 2k_{10}p_{10}}{2|\bar{k}_1||\bar{p}_1|} + \cos \theta_{k_1} \right) \\
&\cdot P_i \cdot \ln\left(\frac{-k_1^2 + 2k_{10}p_{10} + 2|\bar{k}_1||\bar{p}_1|}{-k_1^2 + 2k_{10}p_{10} - 2|\bar{k}_1||\bar{p}_1|}\right)^2 ,
\end{aligned} \tag{26}$$

where

$$P_I = \ln^3\left(\left(1 - \sqrt{Q^2/s}\right)^2\right) - \ln^3(4m_e^2/s) , \quad P_{II} = \ln\left(\frac{(s - 4m_e^2)}{\sqrt{Q^2}(2\sqrt{s} - \sqrt{Q^2})}\right) \tag{27}$$

for the change of variables from Eq.(21) or Eq.(22) respectively. Again $0 < r_i < 1$ for $i = k_1^2, \dots, \phi_{\pi_1}$.

The function, which approximates the peaking behaviour of the matrix element reads

$$F = \left(\frac{1}{P(q_1, q_2)} + \frac{1}{P(q_2, q_1)} + \frac{a}{P_s} \right)^{-1}, \text{ with } P_s = \frac{P_{s,I} + bP_{s,II}}{\frac{3 \ln^2(k_1^2/s)}{k_1^2} + \frac{b}{s-k_1^2}}. \quad (28)$$

The introduced a priori weights a and b , which guarantee the right relative contributions from different generation channels, were set to $a = 1.1$ and $b = 1000$, a choice optimal for DAPHNE energy.

3 The pair production and the radiative return

As the only experiment, which uses the radiative return method without photon tagging is KLOE, we present here the results for DAPHNE energy only. The cross section of the reaction $e^+e^- \rightarrow \pi^+\pi^- + \gamma(\gamma)$ was obtained with the PHOKHARA 5.0 [8] event generator. For the event selection used by KLOE [2] the relative contribution of the pair production to the cross section of the reaction $e^+e^- \rightarrow \pi^+\pi^- + \gamma(\gamma)$ is shown in Fig.2 (left). It amounts up to 1.5% in the vicinity of the production threshold, but it is below 1% in the Q^2 region, where the measurement was performed [2] ($Q^2 > 0.33\text{GeV}^2$).

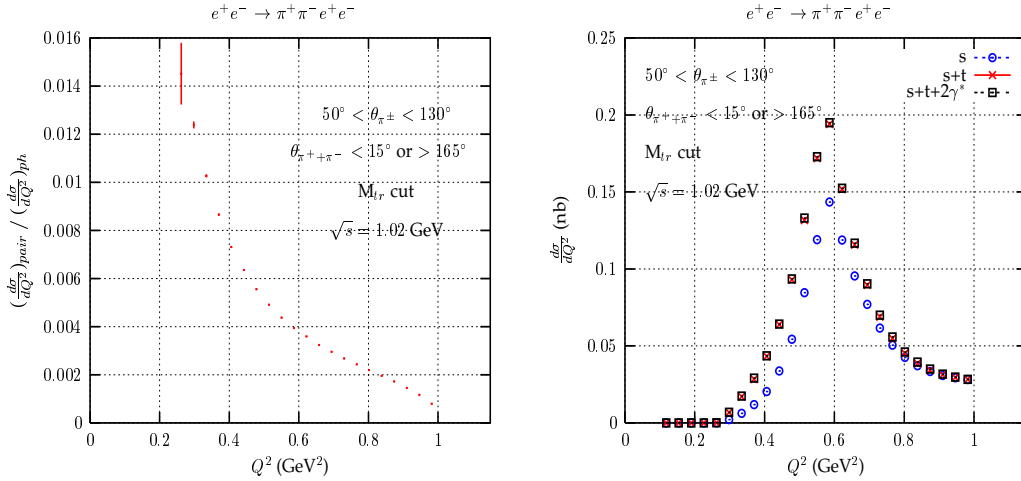


Fig. 2. The ratio of the differential cross sections of the reactions $e^+e^- \rightarrow e^+e^-\pi^+\pi^-$ and $e^+e^- \rightarrow \pi^+\pi^-\gamma(\gamma)$ for KLOE [2] event selection (left) and separate contributions to the cross section of the reaction $e^+e^- \rightarrow e^+e^-\pi^+\pi^-$: s -diagrams from Fig. 1a-1c included; $s+t$ -diagrams from Fig. 1a-1d included; $s+t+2\gamma^*$ -all diagrams from Fig. 1 included (right).

For small Q^2 values the main contribution is given by the t -channel diagrams, while around the ρ resonance the s -channel dominates (see Fig.2(right))

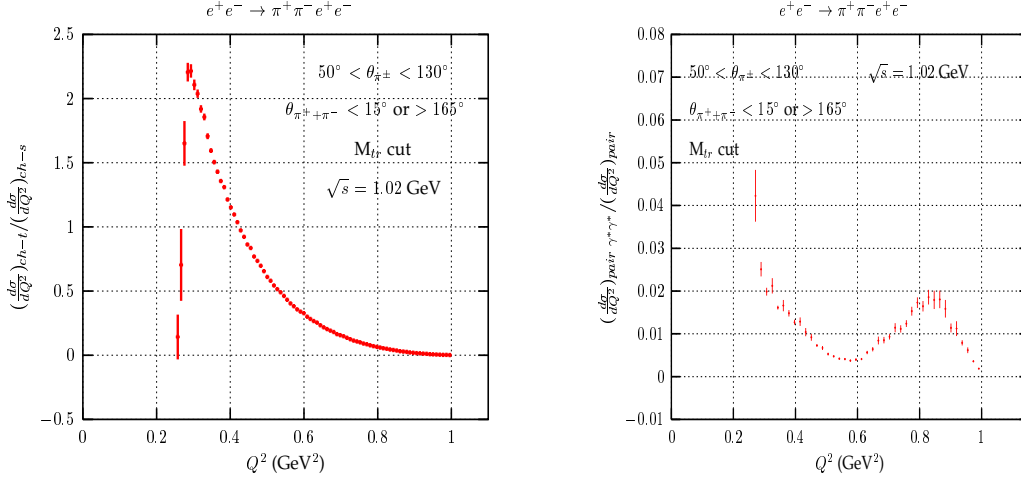


Fig. 3. The ratio of the t-channel and the s-channel contributions to the differential cross section of the reaction $e^+e^- \rightarrow \pi^+\pi^-e^+e^-$ (left); the relative contribution of the photon fusion process to the differential cross section of the reaction $e^+e^- \rightarrow \pi^+\pi^-e^+e^-$ (right)

and Fig.3). In the latter case, as it was shown in [10], the ISR contributions dominate and the FSR is irrelevant. Moreover, the contributions to the cross sections from diagrams from Fig.1c are always small and the two-photon contributions (Fig.1e) are completely negligible for the KLOE event selection as already pointed out in [15] and shown in Fig.3(right). This may not be true for different event selections, as the photon fusion diagrams can give sizable contributions especially in low Q^2 region. An example is presented in Fig.4, where only cuts on pion angles are applied. The pair production cross section can be in this case almost as big as the $e^+e^- \rightarrow \pi^+\pi^-\gamma(\gamma)$ cross section, where the $s + t$ channel diagrams (Fig.1(a-d)) give only up to 3% of the $e^+e^- \rightarrow \pi^+\pi^-\gamma(\gamma)$ cross section [11] and the main contribution is given by the photon fusion diagrams.

In the case of s-channel ISR and the pion pair emission from t-channel Bhabha diagrams a factorization analogous to the one of Eq.(1) occurs, with the radiator function given by QED. As a result, for the case of the KLOE event selection without photon tagging, it is possible to use the radiative return method adding contributions from the photon(s) and the pair production. The pion form factor, to be extracted from the data, is the same in both cases and the radiator function is a sum of both contributions. This procedure will be necessary, when the accuracy of the measurement will be below 1% at low Q^2 values. Alternatively, one can treat the pair production as a background and study carefully the accuracy of its estimation.

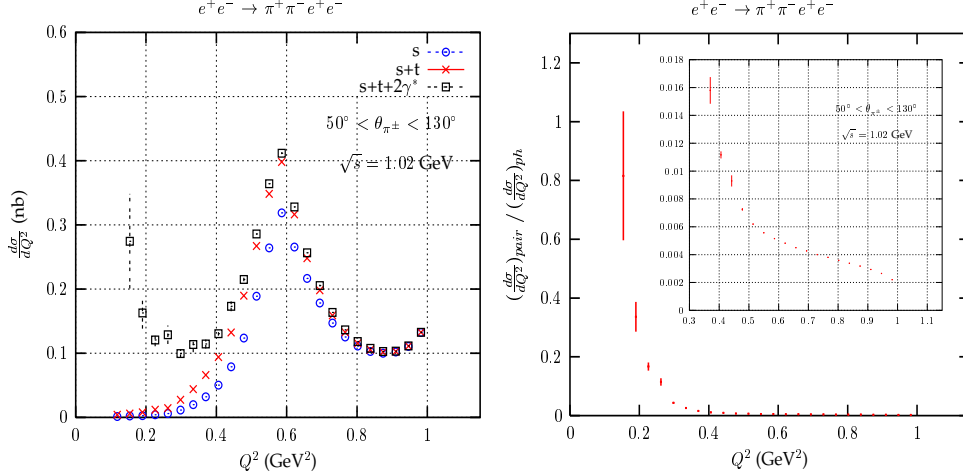


Fig. 4. Various contributions to differential cross sections of the reaction $e^+e^- \rightarrow e^+e^-\pi^+\pi^-$: s – diagrams from Fig. 1a-1c included; $s + t$ – diagrams from Fig. 1a-1d included; $s + t + 2\gamma^*$ – all diagrams from Fig. 1 included (left); The ratio of the differential cross sections of the reactions $e^+e^- \rightarrow e^+e^-\pi^+\pi^-$ and $e^+e^- \rightarrow \pi^+\pi^-\gamma(\gamma)$ (right). In both cases only cuts on pions polar angles are imposed.

4 Conclusions

Basing on the developed Monte Carlo program EKHARA presented in this letter, it was shown that the reaction $e^+e^- \rightarrow e^+e^-\pi^+\pi^-$ may give non negligible contributions to the pion form factor measurement via the radiative return method without photon tagging. For low invariant masses of the two-pion system it is up to 1% for the event selection used in KLOE analysis [2], but it can be substantially larger if some of the cuts, used in the analysis, are relaxed.

5 Acknowledgments

We would like to thank Achim Denig, Wolfgang Kluge, Debora Leone and Stefan Müller for discussions of the experimental aspects of our analysis and TTP of the Univ. of Karlsruhe, where a part of this work was performed, for the kind hospitality.

References

- [1] Min-Shih Chen and P. M. Zerwas, Phys. Rev. D **11** (1975) 58.

- [2] A. Aloisio *et al.*, [KLOE Collaboration], Phys. Lett. B **606** (2005) 12, [hep-ex/0407048].
- [3] B. Aubert *et al.* [BABAR Collaboration], Phys. Rev. D **70** (2004) 072004 [hep-ex/0408078]; Phys. Rev. D **71** (2005) 052001 [hep-ex/0502025].
- [4] M. Davier, S. Eidelman, A. Hocker and Z. Zhang, Eur. Phys. J. C **31**, 503 (2003) [hep-ph/0308213].
- [5] F. Jegerlehner, Nucl. Phys. Proc. Suppl. **131**, 213 (2004) [hep-ph/0312372].
- [6] A. Nyffeler, Nucl. Phys. Proc. Suppl. **131**, 162 (2004).
- [7] G. Rodrigo, A. Gehrmann-De Ridder, M. Guillaume and J. H. Kühn, Eur. Phys. J. C **22** (2001) 81 [hep-ph/0106132]; G. Rodrigo, H. Czyż, J.H. Kühn and M. Szopa, Eur. Phys. J. C **24** (2002) 71 [hep-ph/0112184]; J. H. Kühn and G. Rodrigo, Eur. Phys. J. C **25** (2002) 215 [hep-ph/0204283]; H. Czyż, A. Grzełińska, J. H. Kühn and G. Rodrigo, Eur. Phys. J. C **27** (2003) 563 [hep-ph/0212225]; Eur. Phys. J. C **33** (2004) 333 [hep-ph/0308312]; Eur. Phys. J. C **39** (2005) 411 [hep-ph/0404078]; Phys. Lett. B **611** (2005) 116 [hep-ph/0412239]; H. Czyż, J. H. Kühn, E. Nowak and G. Rodrigo, Eur. Phys. J. C **35** (2004) 527 [hep-ph/0403062].
- [8] H. Czyż, A. Grzełińska, J. H. Kühn and G. Rodrigo, hep-ph/0512180.
- [9] A. Hofer, J. Gluza and F. Jegerlehner, Eur. Phys. J. C **24** (2002) 51, [hep-ph/0107154].
- [10] H. Czyż and E. Nowak, Acta Phys. Polon. B **34** (2003) 5231 [hep-ph/0310335].
- [11] H. Czyż and E. Nowak-Kubat, Acta Phys. Polon. B **36** (2005) 3425 [hep-ph/0510287].
- [12] K. Kołodziej and M. Zrałek, Phys. Rev. D **43** (1991) 3619.
- [13] F. Jegerlehner and K. Kołodziej, Eur. Phys. J. C **12** (2000) 77 [hep-ph/9907229].
- [14] C. Bruch, A. Khodjamirian and J. H. Kühn, Eur. Phys. J. C **39** (2005) 41 [hep-ph/0409080].
- [15] J. Lee-Franzini, talk at Lepton Moments International Symposium, Cape Cod (June 2003), <http://g2pc1.bu.edu/leptonmom/program.html> .